

Hydrodynamic instabilities of viscous coalescing droplets

H. Aryafar and H. P. Kavehpour

Mechanical and Aerospace Engineering Department, University of California, Los Angeles, California 90095, USA

(Received 11 December 2007; revised manuscript received 26 June 2008; published 10 September 2008)

Droplets coalescing at a planar fluid-fluid interface are studied in detail in the Stokes regime with high speed photography. Attention is paid to the expansion of the interfacial bridge, formed between the droplet and interface, as it expands during the process. We report a hydrodynamic instability at the rim of the interfacial bridge. As the rim becomes unstable, it forms a series of tendrils which themselves become unstable and produce micron sized droplets. We show that rim stability depends on drop and medium viscosities as well as the rim geometry.

DOI: [10.1103/PhysRevE.78.037302](https://doi.org/10.1103/PhysRevE.78.037302)

PACS number(s): 47.55.df, 47.61.Ne

The study of coalescing bodies can be traced back as far as the 19th century to the work of Reynolds and Lord Rayleigh [1,2]. Although there have been numerous studies in the last century [3–8], only recently has the technology necessary to fully capture the fluid dynamics of this phenomena been available [9–11]. When a droplet approaches a fluid-fluid interface slowly, the ambient fluid must drain away before the droplet can coalesce. As the layer of the ambient fluid between the drop and the interface becomes thinner, viscous forces dominate, and the drainage process slows. The fluid trapped in between the interface and the surface of the drop is referred to as the interfacial film. Once a critical thickness is achieved, van der Waals force bridges the drop and interface and causes the thin film to rupture. The expansion of the liquid bridge connecting a droplet to the liquid bulk is analogous to that seen in two droplets merging [12].

When studying coalescing fluid bodies, three major parameters to consider are the Weber number $We = \rho v^2 l / \sigma$, the Bond number $Bo = \Delta \rho g l^2 / \sigma$, and the Ohnesorge number, $Oh = \mu / \sqrt{\rho \sigma l}$, where ρ is density, v is velocity, l is the length scale of the coalescing body (in this case the radius of the droplet), σ is interfacial surface tension, $\Delta \rho$ is the density difference between the two fluid bodies, g is gravity, and μ is absolute viscosity. In all of our experiments, the gravitational forces as well as inertia can be neglected ($Bo \ll 1$ and $We \ll 1$). With these external forces being nullified, coalescence is dominated by Oh , which can be considered the ratio of viscous forces to capillary driven inertial forces. The focus of this paper is on the coalescing of droplets with $Oh > 1$. The case of inertia dominated coalescence at flat interfaces, $Oh < 1$, was previously studied by the authors [12,13].

It has been shown that for drop-plane and drop-drop coalescence of low Ohnesorge number, the interfacial bridge radius expands as $r_b = R_{\text{drop}} D^* \sqrt{t/t_i}$, where r_b is the bridge radius, R_{drop} is the drop radius, D^* is a dimensionless prefactor numerically shown to be 1.62, t is time, and t_i is the inertial-capillary time scale defined as $\sqrt{\rho R_{\text{drop}}^3 / \sigma}$ [9,12,14–17]. When $Oh > 1$ (i.e., viscous forces are retarding the coalescence process) it has been shown that the interfacial bridge expands linearly with time, $r_b \sim \sigma t / \mu$, for drop-drop coalescence [14]. A similar scaling was observed when the process of drop-drop coalescence was studied numerically but with the addition of a logarithmic correction factor, $r_b \sim -(\sigma t / \mu) \ln(\sigma t / \mu R_{\text{drop}})$ which is valid for the beginning

stages of rupture [18]. Experimental studies on drop-drop coalescence, however, have not confirmed the logarithmic correction factor [14,17,19], but may not have had the resources to resolve the early stages. It should be noted that a study of soap film rupture inside a viscous medium does show a logarithmic scaling for the rupture velocity [20] which may be due to the inherently thin soap film transitioning to the nonlogarithmic region at further rupture distances.

Our setup employs two immiscible fluids separated by a flat interface. These fluids are housed in a 5 in. \times 5 in. transparent Plexiglas tank that allows any processes within to be recorded with high-speed photography (Phantom v4 and v7, Vision Research, Inc.). The relative densities determine whether the medium is the upper or lower liquid in the system and where the droplet is deposited. In either scenario, even though gravitational forces are negligible during the actual coalescence process, the density deficit draws the droplet to the interface. The high-speed camera is positioned above the tank pointing down if the droplet is in the lower liquid or below the tank pointing up if the droplet is in the upper liquid, see Fig. 1 [21]. This allows for the droplet-interface interaction to be recorded without the droplet ob-

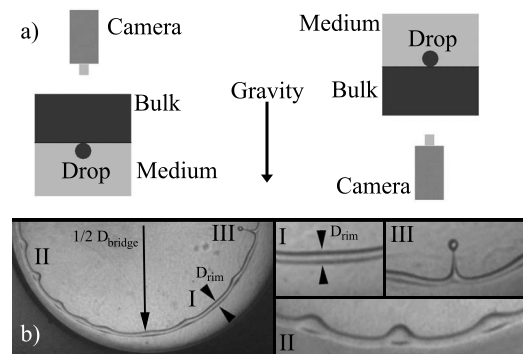


FIG. 1. (a) Two different camera-experiment arrangements based on the relative densities of the fluids. (b) Mineral oil droplet coalescing at a 100 cSt silicone oil-mineral oil interface observed from above the interface viewing downward, top left-hand configuration [12]. I, shows the rim retracting with no apparent instabilities. II, shows beading occurring. III, shows a single bead stretching into a tendril and a droplet being pinched off. The radius of the interfacial bridge is denoted by $D_{\text{bridge}}/2$ and the diameter of the stable rim is denoted by D_{rim} .

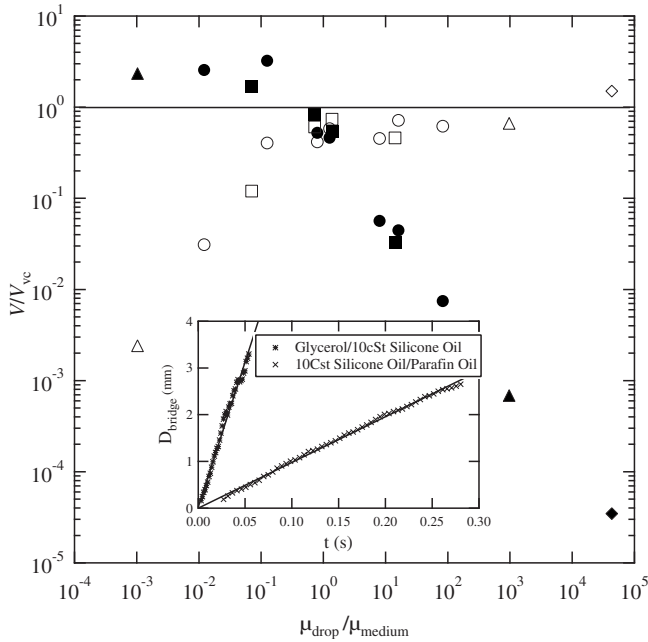


FIG. 2. Retraction velocities scaled using either the medium or drop viscosity scale versus viscosity ratio. Working fluids are glycerol-silicone oil (circles), paraffin oil-silicone oil (squares), water-silicone oil (triangles), and glycerol-air (diamonds). Closed symbols represent scaling with medium viscosity and open symbols represent scaling with drop viscosity. The correct viscosity scale contains the higher of the two viscosities. Inset: The expansion of the interfacial bridge diameter, D_{bridge} , versus time, t , with linear fittings, $D_{\text{bridge}} = V_{\text{vc}} Ca t$.

scuring the view. The details of this setup were shown in our previous presentation [12].

In order to create drops of relatively high Ohnesorge number, fluids of relatively high viscosity were employed, as well as fluid combinations that result in low interfacial surface tension. For the experiments of high viscosity, three fluid pairs were employed: Glycerol and silicone oils of viscosities of 10 cSt, 100 cSt, and 1000 cSt; water and silicone oil of 1000 cSt viscosity; and glycerol droplets in air were also briefly explored. To create low interfacial tension fluid combinations, the above-mentioned silicone oils were used with paraffin oil as the companion fluid. The interfacial tension between these oils is very low ($\sigma = 1.0 \pm 0.1$ mN/m). Interfacial tensions were measured using Du Noüy ring method (DCA-315, Thermo). To increase Ohnesorge number, there also exists the option of drastically reducing the size of the droplet, but this is beyond the abilities of our optical system.

At the onset of coalescence, the radius of the bridge connecting the drop to the bulk was observed to expand linearly with time for all fluid combinations, see inset of Fig. 2. The rate of expansion is normalized using the two possible viscopillary velocity scales, $V_{\text{vc}} = \sigma/\mu_{\text{drop}}$ and $\sigma/\mu_{\text{medium}}$, as shown in Fig. 2. One employs the drop fluid viscosity, while the other uses that of the medium fluid viscosity. For viscosity ratios much less than unity, $\mu_{\text{drop}}/\mu_{\text{medium}} \ll 1$, the correct scaling viscosity is that of the medium. The opposite is true for viscosity ratios greater than unity. Therefore, it is always the higher of the drop and medium viscosities that dominates

the expansion of the interfacial bridge. This leads to a dominant capillary number, $Ca = V/V_{\text{vc}}$, of 0.62 and 2 for $\mu_{\text{drop}}/\mu_{\text{medium}} \geq 1$ and $\mu_{\text{drop}}/\mu_{\text{medium}} \leq 1$, respectively. Capillary number values attained by Aarts *et al.* are 0.55 for a simple pendent-sessile system of silicone oil in air and 0.4 for the liquid phase in a low surface tension colloidal system [14]. Our experimental results agree with experimental work on drop-drop coalescence in that they show no signs of a logarithmic correction factor in the expansion of the interfacial bridge.

Our attention now turns to the instability observed in the retracting interfacial film, shown in Fig. 1(b). The movie of this phenomenon can be found in supplementary material [21]. To clarify, the interfacial film is merely the medium fluid trapped between the droplet and interface, while the interfacial bridge is the fluid bridge connecting the droplet to the bulk fluid below. It is worth noting that the instability in the retracting film does not affect the rate of expansion of the interfacial bridge. This instability has never been reported in viscous drop-drop coalescence experiments [14,17,19] but was predicted by Eggers *et al.* [18]. To the best of the authors knowledge, this instability is not reported in literature involving inertially dominated drop coalescence [5,9,12–16,18,22,23], although a similar instability has been noted in a study on the rupture of soap films in viscous environments [20].

As the interfacial film retracts, in both stable and unstable ruptures, a rim is observed to form at the edge, seen in Fig. 1(b). It is in this rim where the instability manifests itself. Although the thickness of the interfacial film varies from microns to nanometers, the rim is thicker, ranging from hundreds of microns to millimeters. Since direct measure of the interfacial film would be very difficult, we can infer the thickness of the interfacial film by analyzing the rim geometry. Although the rim is assumed to have a circular cross section with a diameter, D_{rim} , for the remainder of the analysis [as shown in Fig. 1(b)-I], its exact geometry cannot be determined with the methods used. Due to the nonuniformity of the film thickness and the asymmetry of the rupture in general, different stability patterns occur along the length of the rim. When rim-bridge diameter or wavelength are mentioned, it should be noted that these are local, instantaneous measurements. Even though the liquid bridge may not be completely circular, $D_{\text{bridge}}/2$ refers to the distance from the point of local measurement of the bridge edge to the point of rupture.

The most basic form of the instability involves the rim forming beads along its length, shown in Fig. 1(b)-II. As these beads of fluid retract with the rim, they can evolve to become tendril-shaped, Fig. 1(b)-III. These long tendrils of the medium fluid will break up into very small droplets. At the completion of coalescence, the original droplet will have completely coalesced, and a crown of tiny droplets, usually microns across, of the medium fluid will be embedded in the opposite side of the interface.

The rim instability is only seen in cases where the Ohnesorge number of the droplet is larger than 0.3 or in other words the viscosity of the droplet is sufficient to bring the coalescence process into the Stokes regime. The interfacial film being trapped in between viscous fluids seems to be

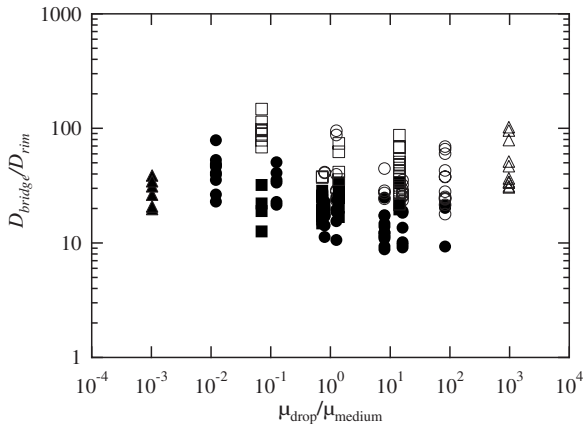


FIG. 3. The aspect ratio of the bridge as a function of the viscosity ratio. The viscosity shows no preference for the instability for values smaller or larger than 1. Working fluids are glycerol-silicone oil (circles), paraffin oil-silicone oil (squares), and water-silicone oil (triangles). Filled markers indicate a stable rim, while unfilled markers represent unstable rims.

essential to the onset of the hydrodynamic instability. This does not mean that the ratio of the drop viscosity to medium viscosity needs to be greater than unity for the instability to occur, as shown in Fig. 3. Rather, the formation of the rim instability occurs for viscosity ratios smaller and greater than unity. This rules out the possibility of the instability being Saffman-Taylor [24] in nature.

An observation made during the experiments was that as the rim becomes thicker, fewer beads form which means the wavelength of the instability depends on the diameter of the rim. It seems that as the rim stretches by the expansion of the interfacial hole, the wavelength of the instability decreases. It is known that the rim by itself, without the attached film, behaves similarly to that of a viscous jet that is wrapped around itself. The critical length at which a jet of viscous liquid will break up due to Rayleigh-Plateau instabilities, L^* , is directly proportional to $D We^{1/2}(1+3 Oh)$, where D is the diameter of the jet [25]. The primary mode for breakup comes from the inertial terms and Ohnesorge number is present to serve as a viscous correction factor. If the circumference of the interfacial hole is taken to be the position of the fluid on the jet, then the ratio of circumference to rim diameter must be greater than L^*/D for the instability to be present as shown in Fig. 4. In addition, the spacing of the pearls approximately follow that of the relationship for the breakup of a fluid column, $\lambda/D_{rim} \approx 5$, where λ is the wavelength of the breakup (inset of Fig. 4) [26]. Although this wavelength can be altered by viscous effects [27], both sets of criteria (viscous jet and fluid column breakup) seem to match experimental measurements.

Keeping in mind that the dominant wavelength of pearl formation follows the breakup of a fluid column, an important parameter for the stability of the rim should be D_{bridge}/D_{rim} , which we refer to as the aspect ratio of the rim. This would be equivalent to the height to circumference ratio of a fluid column if the rim was unrolled from a doughnut into a cylinder. For cases where the rim does not become unstable, a fair assumption would be that the girth of the rim

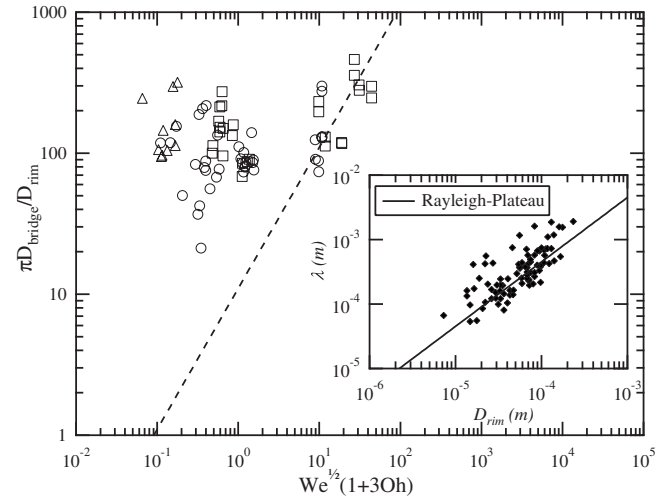


FIG. 4. The ratio of interfacial hole circumference to rim diameter versus $We^{1/2}(1+3 Oh)$. The dotted line represents the breakup of a round linear jet of similar geometry. The pearling instability only occurs near or above the minimum aspect ratio needed for breakup of a round linear jet (showing only points where pearling occurred). Working fluids are glycerol-silicone oil (circles), paraffin oil-silicone oil (squares), and water-silicone oil (triangles). Inset: Wavelength of the instability, λ , plotted versus the rim diameter, D_{rim} , that it occurs at, show similarities to the Rayleigh-Plateau. All length measurements have an error of $\pm 10 \mu m$.

is too large to support a Rayleigh instability along its length. In the event of an instability forming, even though the measurements are taken locally and do not apply to the entire rim, D_{bridge}/D_{rim} should be such that an instability is feasible. If the instability has a dominant inertial based wavelength, then why is the expansion of the interfacial bridge governed by the maximum viscosity? There exists a secondary effect caused by the viscosity of the drop which is essential for the formation of the rim and hence the instability. If we look at the Ohnesorge number of the drop, $Oh_{drop} = \mu_{drop} / \sqrt{\rho \sigma R_{drop}}$, there exists a minimum drop Ohnesorge number (~ 0.3) for which the instability will not manifest itself. This Ohnesorge number is also important for determining the time scales of the coalescence process [13]. It is observed that the wavelength of the instability changes on a much faster time scale than that of the retracting interfacial film. Since the instability is assumed to be inertial in nature, the slow moving, viscous dominated, interfacial film allows for an instantaneous measurement of the rim-instability geometry with confidence that these are not transient values. We also know that the effective Ohnesorge number that governs the behavior of the rim takes the following form: $Oh_{eff} = \mu_{max} / \sqrt{\rho \sigma R_{rim}}$, where μ_{max} is the larger of the two fluid viscosities. Indeed, if the aspect ratio and effective Ohnesorge number are plotted, the stable and unstable regions of bridge expansion are separated, shown in Fig. 5. As the process becomes increasingly dominated by viscous forces, the aspect ratio at which the rim will be susceptible to instabilities decreases.

It may seem counterintuitive that movement towards the Stokes regime would make the onset of the stability more likely. This can be explained by arguing that the beads seen in the rim are originally inertial perturbations which have

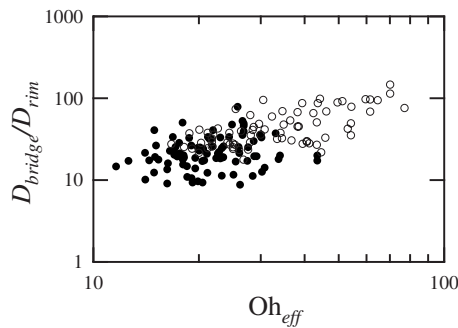


FIG. 5. The effective Ohnesorge, Oh_{eff} , and the aspect ratio of the rim, D_{bridge}/D_{rim} , separate the coalescence process into stable and unstable regions. Open circles represent experiments which produced an instability along the length of the retracting interfacial film. Solid circles represent stable retracting films.

been sustained and amplified by the shear stress from the drop. The rim retraction velocity scales as, $V \sim \sigma/\mu_{max}$, while the shear stress felt tangentially to the surface of the rim scales as, $\tau \sim V/D_{rim}\mu_{drop}$. For cases of viscosity ratio greater than 1, this implies that although an increase in the viscosity of the drop causes the retraction speed of the rim to decrease, the shear stress felt by the rim is unchanged. It is this shear stress along with the extended period of time that is allotted to the slow moving rim that allows the Rayleigh-Plateau disturbances to grow in the Stokes-dominated regime. For cases of viscosity ratio less than unity, an increase in drop viscosity will not change the retraction velocity, but

will increase the shear stress felt at the surface of the interfacial film. The creation of the rim in the retracting interfacial film seems to be essential to the onset of the instability. We know that in the regime that our experiments take place, the retracting interfacial film should not produce a rim in the absence of the drop fluid as is the case for the rupture of a viscous film in air [28]. It must be the viscous effects of the drop fluid which cause the initial formation of the rim and its progression into bead formation, and hence, why the criterion of $Oh_{drop} \geq 0.3$ is necessary.

We have shown the radius of the interfacial bridge connecting a droplet to a flat interface expands linearly with time. The expansion velocity is proportional to the visco-capillary velocity scale only if the higher of the two viscosities are utilized. During the expansion, an instability sometimes forms, which may result in formation of tendrils and eventually the creation of tiny droplets of the medium fluid that are inserted into the bulk drop fluid. This instability has a Rayleigh-Plateau originating wavelength which prorogues along the surface of the rim. The peaks of the wave can then be sustained and/or elongated by the viscous surface stresses caused by the interfacial film retracting between the drop and the fluid bulk. Without the surface stress, the capillary waves would quickly dampen out, as they do for cases of low droplet Ohnesorge number. If the correct rim geometry does not exist, the wavelength of the Rayleigh-Plateau instability will be too great to produce a peak along the length of the rim, and the retracting film will not yield beads or tendrils.

-
- [1] O. Reynolds, Proc. Lit. Phil. Soc. Manc. **21**, 413 (1881).
 [2] L. Rayleigh, Proc. R. Soc. London **28**, 406 (1879).
 [3] R. M. Wiley, J. Colloid Sci. **9**, 427 (1954).
 [4] T. Gillespie and E. K. Rideal, Trans. Faraday Soc. **52**, 173 (1956).
 [5] G. E. Charles and S. G. Mason, J. Colloid Sci. **15**, 105 (1960).
 [6] G. Marrucci, Chem. Eng. Sci. **24**, 975 (1969).
 [7] S. Hartland, Chem.-Ing.-Tech. **42**, 148 (1970).
 [8] D. F. Cooper, B. H. Davey, and J. W. Smith, Can. J. Chem. Eng. **54**, 631 (1976).
 [9] M. M. Wu, T. Cubaud, and C. M. Ho, Phys. Fluids **16**, L51 (2004).
 [10] F. Baldessari and L. G. Leal, Phys. Fluids **18**, 013602 (2006).
 [11] F. Blanchette and T. P. Bigioni, Nat. Phys. **2**, 254 (2006).
 [12] H. Aryafar, A. S. Lukyanets, and H. P. Kavehpour, Appl. Math. Res. Exp. **2000**, 94630.
 [13] H. Aryafar and H. P. Kavehpour, Phys. Fluids **18**, 072105 (2006).
 [14] D. Aarts *et al.*, Phys. Rev. Lett. **95**, 164503 (2005).
 [15] L. Duchemin, J. Eggers, and C. Josserand, J. Fluid Mech. **487**, 167 (2003).
 [16] S. T. Thoroddsen and K. Takehara, Phys. Fluids **12**, 1265 (2000).
 [17] S. T. Thoroddsen, K. Takehara, and T. G. Etoh, J. Fluid Mech. **527**, 85 (2005).
 [18] J. Eggers, J. R. Lister, and H. A. Stone, J. Fluid Mech. **401**, 293 (1999).
 [19] W. Yao *et al.*, Phys. Rev. E **71**, 016309 (2005).
 [20] E. Reyssat and D. Quere, Europhys. Lett. **76**, 236 (2006).
 [21] See EPAPS Document No. E-PLLEE8-78-030809 for a movie of a mineral oil droplet coalescing at a 100 cSt silicone oil-mineral interface. For more information on EPAPS, see <http://www.aip.org/pubservs/epaps.html>.
 [22] G. E. Charles and S. G. Mason, J. Colloid Sci. **15**, 236 (1960).
 [23] Z. Mohamed-Kassim and E. K. Longmire, Phys. Fluids **16**, 2170 (2004).
 [24] P. G. Saffman and G. Taylor, Proc. R. Soc. London, Ser. A **245**, 312 (1958).
 [25] S. Middleman, *Modeling Axisymmetric Flows: Dynamics of Films, Jets, and Drops* (Academic, San Diego, 1995), p. 299.
 [26] J. Eggers, Rev. Mod. Phys. **69**, 865 (1997).
 [27] J. R. Lister and H. A. Stone, Phys. Fluids **10**, 2758 (1998).
 [28] M. P. Brenner and D. Gueyffier, Phys. Fluids **11**, 737 (1999).